Al-Farouk journal of sciences
Volume (2), Issue (3) (JUNE, 2026)
ISSN: 3135-2359

مجلة الفاروق للعلوم
المجلد (2) ملحق العدد 3 يونيو 2026
ردمد: 3135-2359

Spatial and temporal monitoring of surface water area changes in Abhe Lake during 2017-2022 using satellite images and GIS

Dr. Hafid Nanis[1] & Dr. Tarik B. Benomar[2]
[1&2]College of Engineering Technology, Zuwara, Libya
hafidnanis@gmail.com

تاريخ الاستلام: 2026/6/29 تاريخ المراجعة 20/7/ 2026 تاريخ القبول:2026/7/28- تاريخ النشر:10/8/ 2026

Abstract:

Lake Abhe, also called Lake Abbe, is one of six connected lakes that lies on the Ethiopia-Djibouti border. This lake is considered the ultimate destination of the Awash River in the center of the Afar Triangle. It occupies a significant portion of the water resources in the region. The current surface water area of the lake is 347.00 sq.km by the end of this study; however, the surface water area has changed significantly since 1900. Therefore, this study focuses mainly on the continuous monitoring of the surface water changes from 2017 to 2022 using satellite images and Geographic Information Systems (GIS). Operational land images (OLI) Landsat 8 images were processed to estimate the surface water area using a GIS slice tool in ArcGIS to distinguish the water body from the dry land. Some obvious changes have been observed, with significant transformation showing a shrinking trend from the beginning of 2017 to July 2020, followed by an expansion trend from August 2020 to the end of 2022. By comparing the results of this investigation with climate data, it can be concluded that these investigations indicate that the fluctuations in the surface water area in Abhe Lake have been caused by climate changes, specifically the precipitation rate. Overall, these changes should be monitored to ensure the sustainability of water in the lake region.

Keywords: Abhe Lake, GIS, Satellite images, surface water area.

1. Introduction

Lake Abhe is located on the Ethiopia-Djibouti border (Figure 1). Lake Abhe, also known as Lake Abbe, is one of the six connected lakes in the Afar region in Ethiopia, which are Gargori, Laitali, Gummare, Bario, and Afambo from north to south. Many of these lakes are known by alternative names and serve diverse functions, including commercial fishing, recreation, irrigation, and salt extraction (Getahun 2001). In this expanding economic region, surface water reservoirs are vital for the management and economic value of water resources. The lake lies at the Afar triangle, which is a tectonic region in which three plates Nubian (African), Somali, and Arabian are pulling away from the center at different speeds; this place is also called a triple junction in which the three pieces of the Earth's crust are meet. This triple junction between the Red Sea, Gulf of Aden, and East Africa Rift is one of the most active volcanic areas on Earth, as it is part of the East African Rift System (EARS) (Chorowicz 2005; Ring 2014). This place can be considered the lowest area in Africa, located in the sub-Saharan region of Ethiopia. The water surface area in this region depends on rainfall and runoff during the wet seasons from the highlands (Geheb et al.

2003). Over the past decade, human activities and climatic conditions have significantly altered the surface area of these closed water bodies (Hughes RH & Hughes JS, 1992; Houssein, 2010).

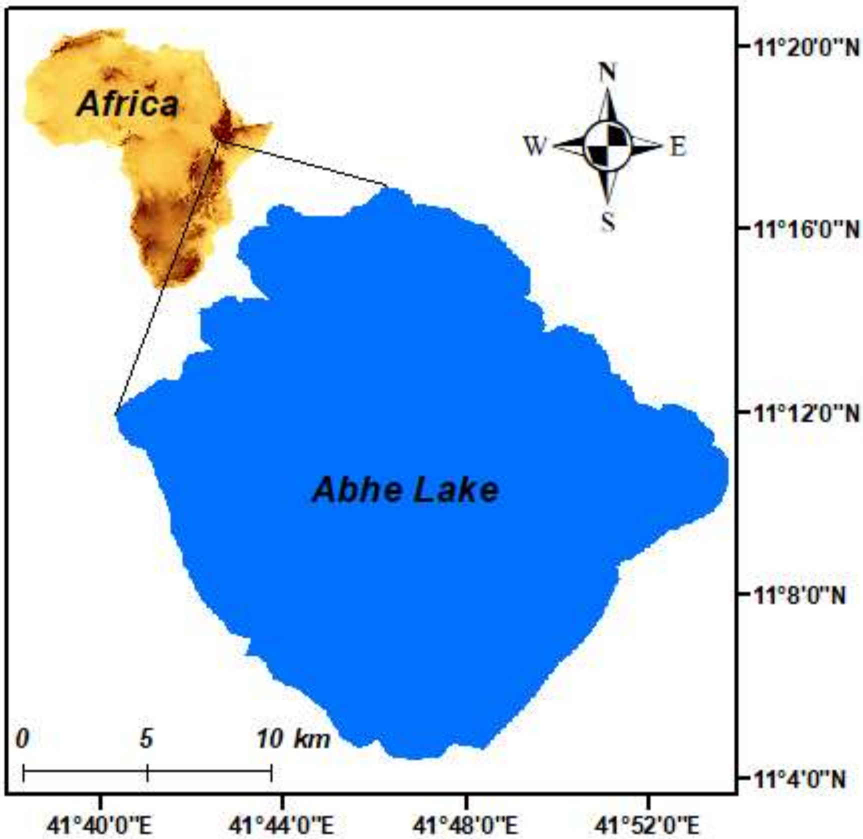

Figure 1. Location map of the Abhe Lake showing its location in Africa.

Lake Abhe is a salt lake with limestone chimneys from where steam emits out and these chimneys reach heights of 50 m (Michael S. 2016). People in the region have established settlements near the lake's shore. This lake can be considered the ultimate destination of the Awash River, which is located at the center of the Afar Triangle. The Awash River, located in the southern part of the region, significantly influences the local surface water area during the rainy season. In recent years, it has been heavily utilized for irrigation (FAO, 1995; Taddese, 2010). Lake Abhe can be on the most inaccessible areas of the earth, and the water itself is known for the flamingos that exist there. Mount Dama Ali (1069 m) as a dormant volcano is located on the northwest shore, while vast salt flats extend along the southwestern and southern shores. Two wadis, Oleldere and Abuna Merekes enter the lake from the west and south, crossing the salt flats beside the Awash River. The lake is situated approximately 240 m above sea level and lies primarily within an arid, hot desert climate zone (BWh), characterized by extreme daytime heat and cooler nights. Summer temperatures often exceed 40 °C, with average highs ranging between 30 °C and 40 °C. During the coldest months, temperatures typically range from 21 °C to 30 °C. Precipitation is minimal and irregular, with an annual average of approximately 172 mm. For the surrounding region, the average temperature and precipitation during the study period (2017–2022) were approximately 23 °C and 22 mm per month, respectively (Climate Research Unit & NCAS).

Across this region, surface water bodies have changed due to a few reasons such as irrigation, and Lake Abhe is not an exception, as irrigation from the Awash River has caused significant water decline in the lake. By the end of this study, the area of the surface water was approximtely 347.00 sq.km, and recent droughts and water extraction from the Awash River for irrigation affected the water level of the lake. The surface water area had been changed since 1940 to two thirds by 1984 (Hughes R.H. 1992). Michael S 2016, states that the water level fluctuating dramatically due to the changes in climate (Michael S. 2016). From 1998 to 2016, the surface water changes had a maximum expansion of 61% between 1998-2002 and a maximum shrinkage of 45% between 2002-2016 as the lake was approximately 344 sq.km in 2002, while it was approximately 190 sq.km in 2016 (Nanis and Aly, 2018).

Long-term fluctuations in lake water levels are a critical issue in Ethiopia, particularly in regions such as Afar where Lake Abhe is located, and poor communities rely on these inland water bodies for salt mining and irrigation. As the region experiences rapid development and population growth, the pressure on its limited water resources continues to intensify. Ethiopia's current water availability is insufficient to meet national food demands (Taddese et al., 2010), and in some areas, impoverished farmers have turned to using municipal wastewater and drainage water from Addis Ababa for irrigation—posing serious health risks (Gizaw, 1996). Therefore, monitoring and assessing changes in the surface water of economically significant lakes is still necessary. However, traditional lake surveys are often expensive, time-consuming, and labor intensive. Geographic Information System (GIS) and satellite images offer a more efficient and cost-effective alternative with broader spatial and temporal coverage. For this reason, satellite data from the Landsat Thematic Mapper (TM), Enhanced Thematic Mapper Plus (ETM+), and Operational Land Imager (OLI) have been widely used in surface water studies (e.g., Work & Gilmer, 1976; White, 1978; Rundquist et al., 1987; Dewidar, 2011; El-Asmar et al., 2013; Kaplan & Avdan, 2017; Policelli et al., 2018). Leveraging these tools, this study integrates Landsat imagery with Geographic Information System (GIS) techniques to continue analyzing Lake Abhe changes from 2017 to 2022. The objectives of this study area as follows:

1. Identify spatial and temporal patterns in surface water fluctuations of Lake Abhe from 2017 to 2022.
2. Quantify lake surface area expansion and shrinkage during the study period.
3. Investigate the contributing factors behind the observed changes in lake size and distribution.

2. Data sources and collection

This study analyzed surface water area changes in Lake Abhe using Landsat 8 Operational Land Imager (OLI) satellite imagery from 2017 to 2022. Only images captured under clear atmospheric conditions or with less than 10% of cloud cover were included. A total of 62 OLI scenes were selected to monitor the lake's surface water extent over the six-year period. Landsat 8 OLI provides 11 spectral bands covering wavelengths from 0.44 to 12.51 µm (Barsi et al., 2014). All satellite data were obtained from the United States Geological Survey (USGS) Earth Resources Observation and Science (EROS) Center, specifically from Path 167 and Row 52, which encompass our study area. The analysis used Collection 2 – Level 2 (On-Demand) products, which were preprocessed for surface reflectance, top-of-atmosphere reflectance, brightness temperature, and spectral indices (Young et al., 2017). The dataset aimed to include one image per month; however, some months were missing because of excessive cloud cover. Table 1 lists the months for which suitable imagery was not available. In addition to satellite data, ancillary information was collected to assess the potential factors influencing surface water changes. This includes climate variables such as temperature, evaporation, and precipitation, which were sourced from the Climate Research Unit at the University of East Anglia.

Table 1. Details of the Landsat images that are missing form this investigation.

Satellite	Sensor	Path-Row	Date	Note
Landsat 8	OLI	167-52	Jun 2017	Missing images due to cloud cover percentage more than 10%
Landsat 8	OLI	167-52	Apr 2018	Missing images due to cloud cover percentage more than 10%
Landsat 8	OLI	167-52	May 2018	Missing images due to cloud cover percentage more than 10%
Landsat 8	OLI	167-52	Oct 2018	Missing images due to cloud cover percentage more than 10%
Landsat 8	OLI	167-52	Apr 2019	Missing images due to cloud cover percentage more than 10%
Landsat 8	OLI	167-52	Jan 2020	Missing images due to cloud cover percentage more than 10%
Landsat 8	OLI	167-52	Mar 2020	Missing images due to cloud cover percentage more than 10%
Landsat 8	OLI	167-52	Apr 2020	Missing images due to cloud cover percentage more than 10%
Landsat 8	OLI	167-52	Dec 2021	Missing images due to cloud cover percentage more than 10%
Landsat 8	OLI	167-52	Aug 2022	Missing images due to cloud cover percentage more than 10%

3. Methods and data processing and spatial analysis

This study used Landsat 8 imagery acquired between 2017 and 2022. All satellite images were automatically pre-processed and radiometrically corrected using the on-demand service provided by the United States Geological Survey (USGS). After correction, the images were projected to the Universal Transverse Mercator (UTM) coordinate system, Zone 37N, based on the World Geodetic System 1984 (WGS84) datum. Remote sensing systems that detect reflected solar radiation, emitted thermal radiation, or active microwave signals are commonly used to delineate open-water features (Paris, 1992). In long-term studies, remotely sensed data acquired in one or more spectral bands—particularly from reflected solar radiation—are widely applied to identify water–land boundaries. Among these, the near-infrared (NIR) band has proven particularly effective for water detection, as water bodies exhibit very low reflectance in this region of the electromagnetic spectrum, in contrast to higher reflectance from vegetation and dry soil (Work & Gilmer, 1976; White, 1978; Rundquist et al., 1987). In this study, the NIR band (Band 5 of Landsat

8, with a wavelength range of 0.851–0.879 μm) is used to extract water features. To ensure consistency and minimize seasonal variation effects, only images captured during spring and summer months are included. Since the study area lies outside high-latitude regions (above 65°N or below 65°S), surface reflectance quality remains unaffected by low solar angle conditions (Young et al., 2017). Water body detection is performed by applying a density slicing technique to the NIR band imagery. This approach classifies pixels into two categories—water and non-water (dry area)—with analysis constrained to lake boundaries using a spatial mask. The classification is based on natural groupings of pixel values, identified using the Jenks optimization method (Jenks, 1967), also known as the Goodness of Variance Fit (GVF). This method aims to minimize the variance within each class while maximizing the variance between classes, thereby achieving an optimal data partitioning. The first step in this classification process involves calculating the Sum of Squared Deviations from the Array Mean (SDAM), defined as follows:

$$SDAM = \sum_{i=1}^{N} \quad (Z_i - \underline{Z})^2 \,, \tag{1}$$

As N is the number of pixels in each satellite image, Z is the value of each pixel, and $\underline{Z}$ is the mean value.

Next, the Sum of Squared Deviations from the Class Means (SDCM) is calculated. This involves computing the squared differences between each pixel value and the mean of its respective class. For each class, the mean pixel value was determined, and the squared deviations of individual pixel values from this class mean were summed. The SDCM is obtained as follows:

$$SDCM = \sum_{j=1}^{K} \quad \sum_{i=1}^{Nj} \quad (Z_{ij} - \underline{Z}_j)^2, \tag{2}$$

As K is the number of desired classes (in our investigation, K represents three classes including deep water, shallow water, and dry area), N_j is the number of values in class j, Z_{ij} belongs to the value in class j, and $\underline{Z}_j$ is the mean value from class j.

Eventually, the Goodness of Variance Fit (*GVF*) is calculated, which ranges from 0 (worst fit) to 1 (best fit), as follow:

$$GVF = \frac{SDAM - SDCM}{SDAM}, \tag{3}$$

This can also be simplified as follow:

$$GVF = 1 - \frac{SDCM}{SDAM}, \tag{4}$$

4. Results and Discussions

Our results demonstrate that the density slicing technique applied to a single Landsat band is effective for accurately estimating changes in surface water area. This approach enables quantitative comparisons across time-series data, facilitating the analysis of water body dynamics in both the spatial and temporal dimensions. However, accurately delineating the precise boundary between water and land remains challenging for small or narrow inland water bodies. All digital image classification methods, including the density slicing technique, rely on grouping continuous pixel values into a limited number of discrete classes. This process can lead to the loss of certain spatial details, particularly in areas with subtle variations in the data. To monitor the surface water changes, a detailed Landsat time-series from 2017 to 2022, including 39 OLI Landsat 8 scenes for Abhe Lake, was created to conduct a comprehensive study as more frequent Landsat images were acquired by Landsat 8 owing to its short revisit time (Figure 2). The figure illustrates the changes in surface water during the study period. Table 2 presents the statistical analysis of surface water area changes in Lake Abhe from 2017 to 2022, revealing that the lake has underwent fluctuations of varying magnitudes throughout the study period. The Lake Abhe has experienced major changes, with a shrinking trend from the beginning of 2017 (185 sq.km) to the beginning of 2020 (136 sq.km), after that an expanding trend to the end of 2022 (348 sq.km). Table 3 highlights the periods of maximum expansion and shrinkage of Lake Abhe from 2017 to 2022. The greatest shrinkage, approximately 26%, was observed between 2017 and 2020, while an increase of approximately 155% was the most significant expansion occurred by the beginning of 2020 to the end of 2022.

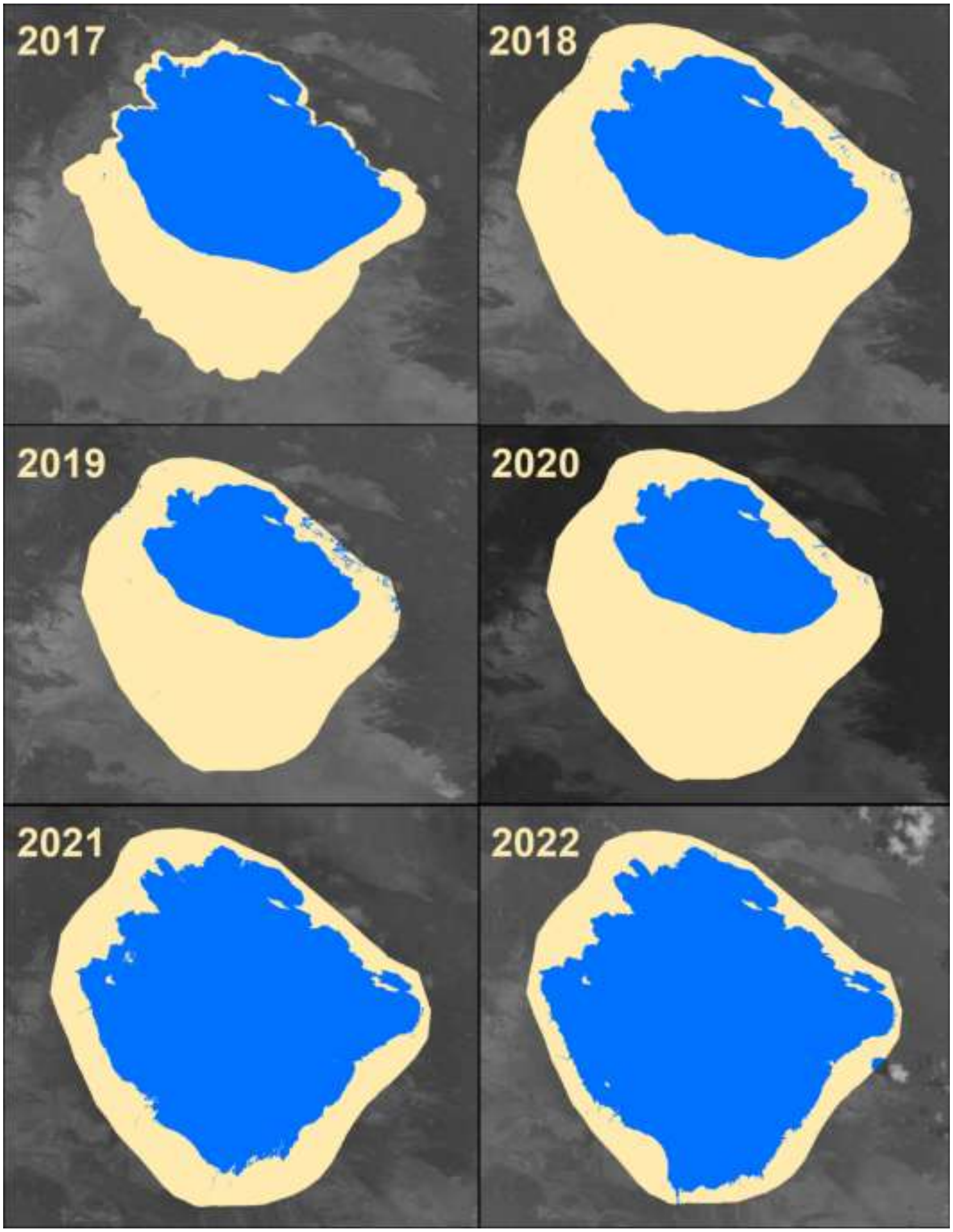

Figure 2. Spatio-temporal evolution of Abhe Lake during 2017-2022. (blue portion shows the surface water area and the Near Infrared band is used as a base map for the lake measurements).

Table 2. Measurements of the surface water area (km^2) for Abhe between 2017 and 2022.

Year	2017	2018	2019	2020	2021	2022
Jan	185	163	148		292	339
Feb	179	162	149	136	301	337
Mar	180	161	151		307	336
Apr	180				293	334
May	175		140	147	303	332
Jun		154	138	144	308	298
Jul	170	155	138	146	282	321
Aug	171	150	142	147	314	
Sep	173	152	139	167	324	349
Oct	171		141	213	332	346
Nov	169	149	139	235	327	348
Dec	167	149	138	262	292	348

Table 3. Maximum expansion and shrinkage in Abhe lake during 2017-2022.

Lake	Shrinkage (%)	Period	Expansion (%)	Period
Abhe	26	2017-2020	155	2020-2022

Lake Abhe is located in the hot desert climate zone (BWh) inside the tropical zone, and the region is defined by very irregular low rainfall and high average temperature, with the hottest month typically above 18° C. Therefore, several climate indices can be used to evaluate changes in surface water, such as drought impact, and each index has advantages and limitations. The annual SPI can't be used in this investigation mainly due to the availability of its calculations for the considered time period over the study area. SPI values reflect the meteorological drought conditions over a period of time for a certain geographic area, whereas negative SPI values indicate rainfall shortfall and positive values indicate rainfall surplus (Cancelliere 2007; WU 2013). It is well known that SPI values are closely related to soil moisture content over short time periods and become more related to groundwater level and reservoir storage over relatively long time periods. Moreover, SPI calculations can be compared across different climatic zones (Vicente-Serrano et al. 2011). The critical limitation of the SPI is that it does not account for changes in evapotranspiration and precipitation intensity; however, alternative indices that account for such factors are not available for our study area and time period.

To determine the reason for these changes, and based on previous study that indicated the effect of the climate change on surface water changes (Nanis and Ali, 2018), climate data were compared to all changes for the analysis. To do so, climate variables of temperature, evaporation, and precipitation obtained from the Climate Research Unit at the University of East Anglia were used in this study to compare them to the surface water changes in the Abhe Lake. Figure 3 shows the relationship between climate data and changes in the surface water area of Lake Abhe during 2017-2022. The average temperature, precipitation, and evaporation, are 23° C, 22.6 mm/month, and 4.9 mm/month, respectively.

Based on these comparing and the diagrams, it can be noticed a positive correlation between Abhe lake shrinking and expansion and low and high precipitation. A visual inspection of Figure 2 shows that the increase in summer precipitation in 2020 and 2021 was always marked by a significant lake area increase in the Landsat image taken in the fall (autumn) of the following years.

As anticipated, high monthly evaporation rates correlated with high monthly temperature rates, and it can be concluded that high temperatures affected the increased evaporation rates in the summer. On average, approximately 72% of the rainfall in the study area is lost through evapotranspiration, 18% is runoff, and only the remaining 10% is rechargeable water (Tadesse et al. 2010).

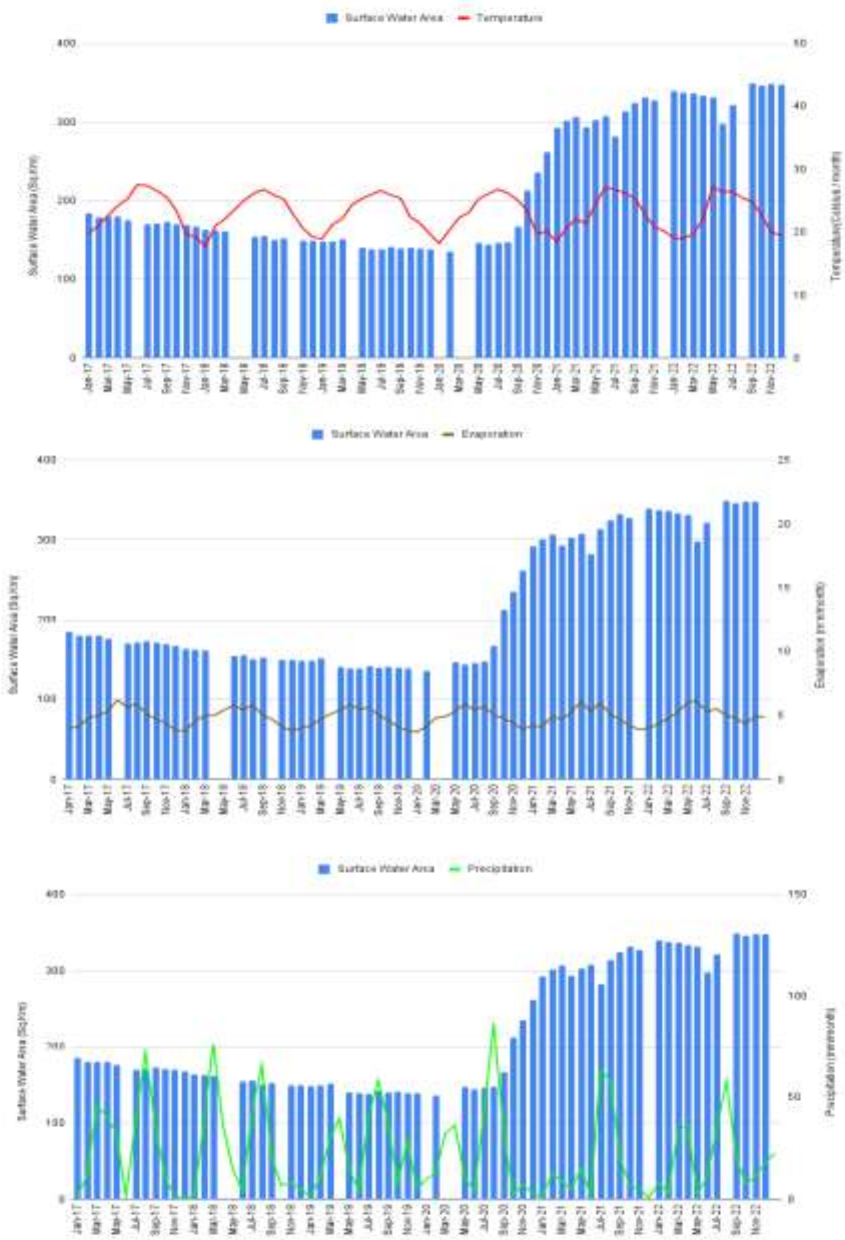

Figure 3. The surface water area of Abhe Lake in comparison to the local monthly climate records of the study period: (a) Precipitation, (b) Evaporation, and (c) Temperature.

The Lake Abhe is one of six connected lakes in the Afar region in Ethiopia, and this lake can be considered the ultimate destination of the Awash River. Thus, surface water changes can be affected by these connections to the nearby lakes and the Awash River, which is connected to the southwestern part of the lake. The river influences the local surface water area during the rainy seasons as it has been used for a few reasons in the region such as irrigation. In addition, the regional population increase in the region may have impacted the consumption of water from the lakes in the region (Ayele et al. 2007). The Awash River Basin has faced land, water, and wetland degradation in recent years, with high population densities in its lower and upper parts (Taddese et al. 2010). This situation has led to an increase in the demand water for essential human needs, including irrigation and grazing; however, it is impossible to quantitatively assess such impact without complete lake records, which are unfortunately not currently available for lakes in the region. Recharge from other inland water bodies may have played a substantial role in increasing the surface water area of Lake Abhe.

Seismic and magmatic activities that have occurred in the region throughout the study period have not been considered, as in the previous study, indicating that there is no clear connection between surface water area changes in Afar lakes and the documented earthquakes and volcanic eruptions. While there were some events in the region during the period time of the previous study, the inspection indicates that there are no noticeable fluctuations in the spatial and temporal patterns of the surface water area that can be aligned with such events during that period (Nanis and Aly 2018).

5. Conclusions

By integrating remote sensing and GIS techniques, this study discovered and continued to monitor changes in the surface water area of Lake Abhe during 2017-2022. The outcomes show that Lake Abhe experienced significant change from the fall of 2020 to the end of the study period, whereas slight changes occurred from the beginning of the study period to the beginning of 2020. Generally, the surface water area in Lake Abha diminished between 2017 to the beginning of 2020, with a shrinking rate of 26%, and then increased significantly with some fluctuations between fall 2020 and end of 2022 whit the greatest expansion of 155% occurred by the beginning of 2020 to the end of 2022. Monthly precipitation is considered the primary factor driving these changes in the surface water of the Abhe Lake. However, recharge from nearby inland water bodies and human activities may also have contributed significantly in the region. This study is expected to provide a foundation for water resource planning and management in rapidly developing regions and across other parts of Ethiopia and Djibouti, particularly during years of above-average rainfall.

Disclosure statement

No potential conflict of interest is reported by the authors.

References:

Ayele A, Jacques E, Kassim M, Kidane T, Omar A, Tait S, Nercessian A, de Chabalier J-B, King G. 2007. The volcano–seismic crisis in Afar, Ethiopia, starting September 2005. Earth Planet Sci Lett. 255:177–187.

Barsi J, Lee K, Kvaran G, Markham B, Pedelty J. 2014. The spectral response of the Landsat-8 Operational Land Imager. Remote Sens. 6:10232–10251.

Cancelliere A, Mauro GD, Bonaccorso B, Rossi G. 2007. Drought forecasting using the Standardized Precipitation Index. Water Resour Manag Dordr. 21:801–819.

Chorowicz J. 2005. The East African rift system. J Afr Earth Sci. 43:379–410.

Dewidar, K. 2011. Monitoring temporal changes of the surface water area of the Burullus and Manzala Lagoons using automatic techniques applied to a Landsat satellite data series of the Nile Delta coast. Mediterranean Marine Science, 12(2): 462-478.

Elwalwa, H. M., Zarig, F. H. A., Murad, M. K. H., & Nashnush, A. N. E. (2026). The role of innovation technology in developing solar energy technologies: challenges and future trends towards sustainable development (literature review). *Al-Farooq Journal of Sciences*, *2*(3), 585-594.

El-Asmar, H. M., Hereher, M. E., & El Kafrawy, S. B. 2013. Surface area change detection of the Burullus Lagoon, north of the Nile Delta, Egypt, using water indices: A remote sensing approach. The Egyptian Journal of Remote Sensing and Space Sciences, 16(1): 119-123.

Geheb K, Yilma D. Abebe, IUCN Eastern Africa Programme, IUCN Wetlands and Water Resources Programme, editors. 2003. Wetlands of Ethiopia: proceedings of a seminar on the resources and status of Ethiopia's wetlands. Nairobi, Kenya: IUCN.

Getahun A. 2001. Lake Afdera: a threatened saline lake in Ethiopia. SINET Ethiop J Sci. 24(1):127-131.

Gizaw, B. 1996. The origin of high bicarbonate and fluoride concentrations in waters of the Main Ethiopian Rift Valley, East African Rift System. Journal of African Earth Sciences. 22(1): 391-402.Hamling IJ, Wright TJ, Calais E, Lewi E, Fukahata Y. 2014. InSAR observations of post-rifting deformation around the Dabbahu rift segment, Afar, Ethiopia. Geophys J Int. 197:33–49.

Hafid Nanis & Mohamed H. Aly. 2018: Desegregation of remote sensing and GIS to characterize fluctuations in the surface water area of Afar Lakes, Ethiopia, Geocarto International, DOI: 10.1080/10106049.2018.1559884

Houssein B. 2010. Geochemistry overview of hot spring from the lake Abhe. Third East African Rift Geothermal Conference. Republic of Djibouti. p. 158–169.

Hughes RH, Hughes JS 1992. A directory of African wetlands. [IUCN, Gland, Switzerland and Cambridge, UK / UNEP, Nairobi, Kenya / WCMC, Cambridge, UK]. pp. 443–447. ISBN 978-2-88032-949-5.

Jenks GF. 1967. The data model concept in statistical mapping: ", International Yearbook of Cartography. 7:186-190.

Kaplan G, Avdan U. 2017. Water extraction technique in mountainous areas from satellite images. J Appl Remote Sens. 11(4): 046002.

Michael Schagerl. 2016. Soda Lakes of East Africa. Springer. p. 8. ISBN 978-3-319-28622-8.

Paris JF. 1992. Remote sensing applications for freshwater systems. In: Firth P, Fisher SG, editors. Glob Clim Change Freshw Ecosyst [Internet]. Springer New York, NY. p. 261–284.

Policelli, F., Hubbard, A., Jung, H., Zaitchik, B., & Ichoku, C. 2018. Lake Chad total surface water area as derived from land surface temperature and radar remote sensing data. Remote Sensing, 10(2): 252.
Ring U. 2014. The East African rift system. ResearchGate. 107:132–146.
Rundquist DC, Lawson MP, Queen LP, Cerveny RS. 1987. The relationship between summer-season rainfall events and lake-surface area. J Am Water Resour Assoc. 23:493–508.
Taddese G, Sonser K, Peden D. 2010. The water of the Awash River Basin a future challenge to Ethiopia. Addis Ababa Ethiopia.
The Climate Research Unit (University of East Anglia) and the UK National Centre for Atmospheric Science (NCAS) (https://crudata.uea.ac.uk/cru/data/hrg/).
Vicente-Serrano, S. M., S. Beguería, J. I. López-Moreno. 2011. Comment on "Characteristics and trends in various forms of the Palmer Drought Severity Index (PDSI) during 1900–2008" by Aiguo Dai, J. Geophys. Res. 116: D19112.
White M. 1978. Reservoir surface area from Landsat imagery. Photogramm Eng Remote Sens. 44:1421–1426.
Work EA, Gilmer DS. 1976. Utilization of satellite data for inventorying prairie ponds and lakes. Photogramm Eng Remote Sens. 42(5):685-694
WU Man-chi. 2013. A brief introduction to Standardized Precipitation Index (SPI). [accessed 2018 Jun 13]. Available from: http://www.hko.gov.hk/education/edu01met/wxphe/ele_spi_e.htm
Young NE, Anderson RS, Chignell SM, Vorster AG, Lawrence R, Evangelista PH. 2017. A survival guide to Landsat preprocessing. Ecology. 98:920–932.